Nat. Hazards Earth Syst. Sci. Discuss., 3, 1231–1268, 2015
www.nat-hazards-earth-syst-sci-discuss.net/3/1231/2015/
doi:10.5194/nhessd-3-1231-2015

Natural Hazards and Earth System Sciences
Discussions
Open Access

An approach to build an event set of European wind storms based on ECMWF EPS

R. Osinski[1], P. Lorenz[2,1], T. Kruschke[3,1], M. Voigt[4,1], U. Ulbrich[1], G. C. Leckebusch[5,1], E. Faust[6], T. Hofherr[6], and D. Majewski[7]

[1]Institute of Meteorology, Freie Universität Berlin, Berlin, Germany
[2]Meteo Service Weather Research GmbH, Berlin, Germany
[3]GEOMAR Helmholtz Centre for Ocean Resarch Kiel, Kiel, Germany
[4]GFZ German Research Centre for Geosciences, Potsdam, Germany
[5]School of Geography, Earth and Environmental Sciences, University of Birmingham, Birmingham, UK
[6]Munich Re, Munich, Germany
[7]German Weather Service, Offenbach, Germany

Received: 12 January 2015 – Accepted: 26 January 2015 – Published: 9 February 2015

Correspondence to: R. Osinski (robert.osinski@met.fu-berlin.de)

Published by Copernicus Publications on behalf of the European Geosciences Union.

Abstract

The properties of European wind storms under present climate conditions are estimated on the basis of surface wind forecasts from the European Center of Medium-Range Weather Forecast (ECMWF) Ensemble Prediction System (EPS). While the EPS is designed to provide forecast information of the range of possible weather developments starting from the observed state of weather, we use its archive in a climatological context. It provides a large number of modifications of observed storm events, and includes storms that did not occur in reality. Thus it is possible to create a large sample of storm events, which entirely originate from a physically consistent model, whose ensemble spread represents feasible alternative storm realizations of the covered period. This paper shows that the huge amount of identifiable events in the EPS is applicable to reduce uncertainties in a wide range of fields of research focusing on winter storms. Wind storms are identified and tracked in this study over their lifetime using an algorithm, based on the local exceedance of the 98th percentile of instantaneous 10 m wind speed, calculating a storm severity measure. After removing inhomogeneities in the dataset arising from major modifications of the operational system, the distributions of storm severity, storm size and storm duration are computed. The overall principal properties of the homogenized EPS storm data set are in good agreement with storms from the ERA-Interim dataset, making it suitable for climatological investigations of these extreme events. A demonstrated benefit in the climatological context by the EPS is presented. It gives a clear evidence of a linear increase of maximum storm intensity and wind field size with storm duration. This relation is not recognizable from a sparse ERA-Interim sample for long lasting events, as the number of events in the reanalysis is not sufficient to represent these characteristics.

Title Page
Abstract Introduction
Conclusions References
Tables Figures
◄◄ ►►
◄ ►
Back Close
Full Screen / Esc
Printer-friendly Version
Interactive Discussion

1 Introduction

According to the records of insurance and re-insurance companies, wind storms are the most costly natural hazards in Europe (Münchener Rückversicherungs-Gesellschaft, 2011). Fortunately, the most extreme events occur very rarely, but this makes it difficult to estimate their recurrence periods and other statistical characteristics, which can only be estimated with large error bars assigned to them (cf. Della-Marta et al., 2009). Studies estimating these parameters make use of reanalysis and station-data (e.g. Della-Marta et al., 2009; Hofherr and Kunz, 2010) or climate simulations (e.g. Leckebusch et al., 2006). Most recently, a catalogue of damaging European wind storms was produced by Roberts et al. (2014), based on the ECMWF ERA-Interim reanalysis. As one quintessence of this study, it can be said that the EPS provides a reasonable opportunity to enlarge such a catalogue substantially. Statistical models like the random walk or Markov Chain Monte Carlo models are often used to extend samples for the estimation of the recurrence of severe storm events or extreme wind speed with return periods of above 1000 years (e.g. Dukes and Palutikof, 1995). The principal idea to use the EPS, for the same purposes, instead, is the fact that all EPS events are fully based on a physical model, which has the big advantage of a good consistency and coverage of the potential storm related risk. In a statistical sense, observations represent the realized reality. Ensemble forecasts as part of the regular weather forecasts demonstrate that individual weather events could have developed differently, starting from basically the same initial weather conditions. In this sense, observations do not provide information on potential alternative developments that could have been become reality with a similar probability.

Studies on the EPS are mainly focused on the quality of the prediction. An example of such a study related to European winter storms can be found in Buizza and Hollingsworth (2002), where the focus lies on the predictability of the heavily impacting winter storms of the year 1999. Froude (2006, 2009) have analyzed the predictability of storm tracks and extratropical cyclones using a cyclone tracking algorithm by Hodges

(1994). Froude and Gurney (2010) were focusing on the application of the EPS for the oil and gas industry. Output of the ECMWF EPS in an impact based study was already used for estimating the range of potential storm surge events at the German bight (Koziar and Renner, 2005). The small area investigated in this study is, however, not representative for winter storms in Europe. The current study aims at assessing climatological properties of European winter storms, produced by the operational ECMWF Ensemble Prediction System. Such an approach requires minimizing the effects from inhomogeneities in the EPS introduced by the regular updates of this operational system. They could produce systematic deviations from observed storms, the latter being represented by the ERA-Interim reanalysis in our study. Beyond these changes, there could be systematic forecast lead time dependent trends in the EPS dataset, affecting storm characteristics like severity, duration or the affected areas. Jumps and trends as well as biases must be initially addressed in order to carry out climatological investigations.

2 Data

Instantaneous 10 m wind speed data at different archiving time steps as mentioned farther below are considered. The area of investigation covers the Atlantic–European region reaching from 40° W to 40° E and 25 to 80° N. For part of the studies in this paper, the entire Northern Hemisphere was used in order to avoid boundary effects. Used is an extended winter season from September to May.

2.1 ECMWF ERA-Interim

An archive of 6 hourly ERA-Interim reanalysis data (Dee et al., 2011) is used. At the time the current study was performed, data before the year 1989 were not available, so that the period considered is 1989 to 2010. ERA-Interim uses the 4D-Var assimilation scheme and the IFS forecasting system release Cy31r2 at a horizontal spectral resolution of T_L255. The same system release was operational from 12 December 2006 until 05 June 2007, but with horizontal resolution of T_L399 (for details refer to Palmer et al., 2007).

2.2 ECMWF ensemble prediction system EPS

This section provides some relevant aspects about the ECMWF EPS. A more detailed description of the EPS can be found in Palmer et al. (1992, 2007) and Molteni et al. (1996). The Ensemble Prediction System of the ECMWF became operational in December 1992 (see Table 1 for an overview). Initially, 32 perturbed forecast members (based on the method of singular vectors) plus one control forecast (not perturbed against the original analysis, but using the EPS model system instead of its deterministic counterpart) were produced. The number of perturbed ensemble members was increased to 50 in December 1996. Since October 1998, part of the EPS runs are produced including perturbations in the model physics. With increasing computing power, continuous upgrades of the system lead to improvements in the forecast skill (cf. Palmer et al., 2007). The horizontal resolution was increased from T63 to T_L159 (12.1996), T_L255 (11.2000), and T_L399 (02.2006) to T_L639 (01.2010). The resolution of the singular vectors was increased from T21L31, over T42L31 (03.1995), T42L40 (10.1999) to actually T42L62 (02.2008) (Palmer et al., 2007). Changes in the data assimilation scheme (Rabier et al., 2000; Mahfouf and Rabier, 2000; Klinker et al., 2000) from 3D-Var to 4D-Var were introduced in November 1997 (cf. Bouttier and Rabier, 1997). The EPS integration time is 15 days, but after 10 days of forecast the horizontal resolution is decreased. Since March 2003, the system is initialized twice a day, at 12:00 and 00:00 UTC. In order to take the major changes into account, the dataset was split into periods with constant horizontal resolution (Table 1). Data used in this study cover the period until 25 January 2010, thus excluding the latest period with T_L639 resolution. Depending on the period, the EPS data are available in 12, 6 and 3 hourly temporal resolution. As ERA-Interim is only available in 6 hourly resolution, the EPS data with a 3 h resolution were used in subsets of 6 hourly resolution again. For the 12 hourly data, ERA-Interim was also used in this temporal resolution.

3 Methods

3.1 Identification and characterization of storms in mid-latitudes – wind tracking

For the identification and characterization of European winter wind storms, an impact related wind tracking algorithm developed by Leckebusch et al. (2008) is used. It identifies grid points belonging to wind storms by searching for spatial clusters of grid points (extending over an area of at least $1.6 \times 10^5\,\mathrm{km}^2$) where the local 98th percentile of wind speed is exceeded. The choice of the 98th percentile is motivated by the relevance of this threshold for storm damages (Klawa and Ulbrich, 2003). The identified clusters are connected to a track using a nearest neighbor criterion. The maximum distance allowed to connect two clusters to a windstorm-track is limited by an assumed maximum wind field propagation velocity of $120\,\mathrm{km\,h^{-1}}$. In the present study a minimum lifetime of 24 h of an identified windstorm must be fulfilled, equivalent to 3 archived time steps for the 12 h temporal resolution and 5 time steps for 6 h resolution periods (Table 1). By summing the cube of the 98th percentile exceedances belonging to a track an objective storm severity measure is determined. This measure, called Storm Severity Index (SSI), is calculated for each storm over all time steps t and grid points k affected:

$$\mathrm{SSI} = \sum_t^T \sum_k^K \left[\left(\max\left(1, \frac{v_{k,t}}{v_{\mathrm{perc},k}}\right) - 1 \right)^3 \times A_k \right]. \tag{1}$$

3.2 Homogenization of the EPS

The improvements introduced into the operational EPS system mentioned above will affect the results of the tracking procedure in different ways, but a main impact is due to the changes in spatial and temporal resolution. Our approach is to handle these changes as follows: first, the threshold value required for the tracking algorithm has to be identified for each sub-period. Identification and tracking of the wind fields is performed for each period with a specific spatial EPS resolution, thus avoiding interpolations of the wind fields. For the estimation of SSIs according to Eq. (1) we apply a two step procedure. First, the 98 % quantiles of each sub-period are homogenized towards a common basis, using the ERA-Interim data set as a reference. We call this "climatological scaling" (see Sect. 3.2.1). As the excess over the 98 % quantile used for quantifying storm intensity can also be affected by the inhomogeneities, the quantile-quantile mapping approach (cf. Boé et al., 2007; Maraun, 2013) is used in a second step (see Sect. 3.2.2). A quantile-quantile mapping for the different periods without previous climatological scaling is not suitable, as it would completely remove the (real) climate variations.

3.2.1 Climatological scaling

Subdividing the EPS dataset into periods which are homogeneous in terms of the horizontal resolution of the model system (see Table 1) reflects the finding that different resolutions of the EPS system produce different wind speed biases and, as a consequence, biases in SSIs, storm duration and size. Differences in wind speed characteristics for the periods considered can, however, also originate from climate variability. The latter becomes evident when the ERA-Interim data is used for estimating this threshold for the whole period and for the same sub-periods: Fig. 1 shows 98th ERA-Interim percentiles using all land grid points in the Atlantic European area chosen. Land grid points are shown, as the major interest is related to storm damages over land, but the method is applied on all individual cells of the entire grid. The estimates for the four sub-periods vary against the percentile computed for the complete period 1989 to 2010. The percentiles of the EPS versions with coarser horizontal resolution are found to be lower than those with higher resolution. The effect from T_L159 to T_L255 is much stronger than from T_L255 to T_L399. Note that for this intercomparison an interpolation towards the ERA-Interim grid had to be performed. The correction factor for the 98 % quantile of each grid cell is computed taking the factor due to climate variation (as estimated from ERA-Interim) into account.

3.2.2 Scaling of exceedance

After climatological scaling of the wind speed, the percentiles exceeding the 98th one still differ between the sub periods, as shown in Fig. 2. The presented differences in the tail seem to be very small, but as the cubic of these values is used and summed over a larger quantity of grid cells for the SSI calculation, cf. Eq. (1), they are impacting the results. A quantile-quantile mapping is for this reason used. After both climatological scaling and quantile-quantile mapping, the ERA-Interim 98th percentile and the exceeding wind speeds mapped on the ERA-Interim distribution can be used for the SSI calculation in every sub-period.

4 EPS storm validation

4.1 Spin-up effects, threshold and diurnal cycle

Even though spin-up effects in numerical simulations are well known, their magnitudes in the ECMWF EPS have not been a major issue in scientific literature. An exception is the report by Lamquin et al. (2009) focusing on humidity in the upper troposphere. Results of a search for a systematic variation of 98 % quantiles of wind are given in Fig. 3 for the T_L159, T_L255 and T_L399 resolutions. Average values over all land and all sea boxes in the area considered have been computed for archiving steps of the forecasts. For both land and sea grid points a small initialization effect in the first 6 to 12 h of the forecasts becomes visible. The percentile value in the T_L159 resolution over land, for example, is about 0.5 $\mathrm{m\,s^{-1}}$ higher during the first one to two archiving time steps then subsequently. Over sea, there seems to be an effect with opposite signature (lower initial values) in the first 12 to 18 forecast hours. The data for T_L399 over sea show the same initialization effect. The dominant feature in Fig. 3 is, however, a diurnal cycle with an amplitude of about $1\,\mathrm{m\,s^{-1}}$ over land. Maxima occur at the forecast time steps valid noon (12:00 UTC). Note that a corresponding cycle is also found in the ERA-Interim data, with about the same amplitude (not shown). Conventional observations confirm that the daily cycle in the 10 m wind speed over land is a realistic feature (Lapworth, 2008, 2012). The EPS with T_L255 is characterized by an interfering daily periodicity and an 18 h periodicity. As the daily cycle is small over sea, the 18 h periodicity is well visible in Fig. 5e. The irregular behavior of the EPS with T_L255 resolution is apparently related to the stochastic perturbations of the model physics used during the respective period as the unperturbed control forecast produces a regular daily cycle (without figure). A more thorough investigation of the 18 h cycle is beyond the scope of the present paper. We have not attempted to remove it from the investigation, but comparing the windstorm statistics for this EPS resolution with the other periods we found no evidence for a systematic effect.

4.2 Modifications of observed storms in the EPS: storm "Emma"

Different EPS members started at different lead times will produce modifications of observed storm events in terms of their genesis time, track, and intensity. Before considering the respective statistics for the whole time series, we consider the storm event named[1] "Emma" (28 February 2008) in more detail. At a lead time of 6 h, all of 50 EPS runs produce a storm fulfilling our criteria that can be assigned to the observed one (Fig. 4a). The majority of the simulated events are weaker than the intensity computed from ERA-Interim, but for 12 members the simulated storm is stronger than observed. At a lead time of 90 h, taken as a second example (Fig. 4b), in several runs no storm is found. One member, however, produces a storm of about double the observational SSI. The variations in SSI originate from variations in the intensity at individual grid

---

[1] Names are given by the Institute of Meteorology of Freie Universität Berlin.

points, in area and in storm lifetime, as depicted in Fig. 5 for the 6 h lead time. The track of “Emma” in ERA-Interim and in the individual EPS members (Fig. 6) is found by identifying a storm core from the weighted local SSI contributions of all storm grid points at a time step, and connecting the centers from different time steps (Leckebusch et al., 2008). While in many other cases the observed storm is found close to the centre of the EPS ensemble member storms, all EPS tracks of “Emma” at this lead time are located northward of the ERA-Interim storm (Fig. 6a). For the 90 h lead time (Fig. 6b), the spread between the modified Emma tracks is larger. A notable feature of “Emma” is the fact that the observed “Emma” tends to be at the border of the EPS ensemble also for the long lead time. SSI values for all events detected in ERA-Interim and the EPS (with lead times between 6 and 90 h) over the period 2001 to 2010 are shown in Fig. 7. Over the entire period, the range of SSI in the EPS is much larger than in ERA-Interim. This is partly due to the definition of the SSI, using cubic exceedances. As the motivation for the SSI definition is damage potential, the additional events help to better estimate potential storm risks for Europe, in particular with respect to the occurrence of the most extreme storms.

4.3 Comparison of storm properties in the EPS and ERA-Interim

In order to compare the entire ensemble of storms in the EPS with those detected in the ERA-Interim dataset, events not entirely captured in a forecast must be excluded. They would erroneously be taken as short(er) living storm events. This situation may be present if a storm is detected at the initialization time. In this case, it may have existed before, but could not be tracked on the basis of the driving data. Removing all storms existing at the start of the forecast, however, allows the full range of storm durations to enter the statistics without a bias. A similar kind of problem would occur with storms existing at the end of the 10 day forecast time. Here, the same solution cannot be applied as it would prefer short duration storms for genesis occurring rather late in the forecasted period. We decided to restrict the evaluated storms to those generated at a maximum of 6 days after forecast initialization, leaving 4 days for a maximum duration. There is still a problem with storms lasting 4 days or longer. According to ERA-Interim, only 0.8 % of storms are this long-lasting, and only a part of them (namely, those generated at one of the time steps just before the 6 day limit) are affected. We expect the impact on the results to be small. Also, the choice of 6 days is motivated in the fact that it leads to an equal frequency of evaluated time steps at 0, 6, 12 and 18 h forecast time, thus ameliorating the effects of the 18 h periodicity in intensities mentioned earlier.

Storm properties in the EPS compared to ERA-Interim

The average number, size and duration of storm events per year found in the four different time periods characterized by the specific EPS resolutions is given in Table 2, both for the EPS and ERA-Interim. The number of events in the EPS is the ensemble average over all available ensemble members, initializations per day, and over the forecast length limited to storms lying inside the described six day window (cf. Sect. 4.3). This number can thus be directly compared to the ERA-Interim values given in the same table. The respective values are similar between the two datasets, meaning that the storm properties in the EPS ensemble average are in good agreement to ERA-Interim. In order to compare the severity distributions of the EPS and ERA-Interim events, seven severity classes were formed making sure that a reasonable number of events in each of the classes permit statistical tests. Sub periods with constant horizontal resolution of the EPS are again distinguished. Note that the SSI values calculated from data with twelve hourly resolutions (T63 and T_L159) are expected to be lower than those from six hourly resolutions (T_L255 and T_L399) (Fig. 8) due to the additional time steps included for the latter. It can be seen how the results of the wind tracking differ for the EPS without using any scaling technique, using only the climatological scaling, the scaling of exceedance or both together. Using both scaling techniques, the severity distributions of the EPS and ERA-Interim are comparable for all four sub periods. As it is difficult to evaluate the benefit from the scaling techniques visually, a normal distribution was fitted to the logarithmic of the SSI. The Anderson–Darling test indicates that the logarithmic of the SSI is normal distributed. The benefit from the scaling techniques is illustrated in Fig. 9. Looking for the raw EPS data in T_L399 resolution, they concord better with ERA-Interim than the data in T_L255. The effect of the climatological scaling is relatively small. Using both scaling techniques together, the distributions between the EPS and ERA-Interim look very similar. The fit parameters are shown in Table 3. Errors of the parameters are very small in the EPS case due to its very large sample. The mean and SD lies in between the error resulting from ERA-Interim. This means that the EPS ensemble mean represents well the storm climate, which can be found in ERA-Interim. Storm representations in the EPS and ERA-Interim with comparable SSI values show in the average comparable storm duration as well as the storm size (without figure).

5 Spatiotemporal EPS storm properties

5.1 “Pure” and “modified” EPS storms

Most considerations in this paper are based on the imagination that the EPS produces modifications of storms in the real world (subsequently called “modified EPS storms”), or, for some ensemble members, low windspeeds and thus no storm at all. However, the EPS can produce storm events that have no real world counterpart. As for statistical investigations independent and identically distributed (iid) random variables are necessary, such “pure” events are particularly interesting, because they can increase the sample of independent events. Figure 10 shows a sketch of the definition of “pure” and “modified” storms in this study. To identify “pure” EPS storm events, events are searched for which no simultaneous counterpart can be found in ERA-Interim. We also regard events as “pure” if there is a spatial distance of more than 1500 km between contemporaneous events, as this is a typical synoptical scale of the investigated phenomena.

5.2 EPS storms during the forecast time

Using the aforementioned method to separate "pure" and modified storms, it can be assumed, that close to the initialization time almost only modified storms can be found in the EPS (Fig. 11). All ensemble members are likely to produce the storm that actually occurred, even if properties like size and duration as well as severity vary between the different realizations. For long lead times however, there is an increased number of "pure" EPS storms (grey lines in Fig. 11). The example of storm Emma illustrates that for longer lead times, a number of ensemble members do not show the storm at all, and a larger variability can be found in the intensities. Note that the average number of all storms in the EPS is nearly constant over the forecast time in spite of the small variation in the percentile values (Fig. 3) over forecast time. This number is similar to its ERA-Interim counterpart, supporting our approach to use the individual period's own percentile for storm identification. A diurnal variation in the number of storms related to the diurnal variation in the 98th percentiles (Fig. 3) is reflected in Fig. 11. As the percentile values used for the wind tracking are based on all data, its values lie between the minimum and maximum value of the 6 hourly or 12 hourly resolution. As at 12:00 UTC the 98th percentile value is above the 98th percentile of the entire dataset, the probability of an exceedance at this time of the day is larger than for the other times. For this reason the number of both first and final storm track detections is larger at 12:00 UTC than for the other times.

5.3 Spatial distribution of storms

In order to investigate whether there is a difference in the spatial distribution of European winter storms between ERA-Interim and the EPS, the affection of each grid cell by all detected storms per EPS sub period is computed. The footprint (region of grid cells which is affected by a storm) of each detected storm is analyzed, and for each grid cell the number of footprints affecting this particular grid cell is counted. For comparability the area affections for ERA-Interim are calculated for the same time frames as the EPS sub periods. The results for the ERA-Interim and EPS T_L255 resolutions have identical grid points and are thus comparable without interpolation. For the comparison for the EPS with T_L399 resolution, the result for ERA-Interim was interpolated to this resolution. The entire Northern Hemisphere was used for the tracking to avoid boundary effects caused by a limitation of the area. The basic distribution of the affections is similar in ERA-Interim and the EPS. The lower number (300 times; EPS with 50 member lasting over 6 days) of events available in the observational data causes a much noisier distribution than what is obtained from the EPS. There are local maxima in ERA-Interim for example over North Africa and the Mediterranean which the forecast model is not able to reproduce.

5.4 “Modified” vs. “pure” EPS storms

The interest in “pure” EPS storms is originated in the wish to find events which are independent to modifications of ERA-Interim storms. Using the same procedure as in the section before to determine the spatial affections, but only for footprints of “pure” EPS storms, defined after the method explained in Fig. 10, the results are shown in the Fig. 13 for the EPS with T_L255. Over the Atlantic the number for the “pure” EPS storms is lower than over North Africa and Eastern Europe. The major track of the storm systems is not so strongly affected by “pure” EPS storms as the regions where storms appear less frequently. This has the consequence that the use of “pure” EPS storms as a supplemental amount of events for increasing an independent sample of “modified” storms leads to a bias in the spatial distribution of storms. Using the presented method, the dependency between events to create an iid-sample is defined by a comparison to ERA-Interim. Another feasible approach is to use a matching criterion in between all of the EPS events.

5.5 Storm intensity vs. duration

A benefit of storm statistics based on the EPS instead of Reanalysis is the larger number of storms available for statistical studies of typical mid-latitude storms. The Fig. 14 shows a clear correlation between the storm duration and the maximum wind field size. For storms with duration of up to 54 h, ERA-Interim shows a comparable picture to the EPS. This can be explained by the fact that the number of observed storms of this time scale is large enough to provide a reliable statistic. The EPS indicates that the average spatial growth of storms is independent of their duration, while the duration determines the maximum extension. For long lasting events there seems to be an asymmetry between the growth and the decline, where the growth seems to be faster than the decline. With respect to storm severity, a similar interdependence is found (Fig. 15). Again, the intensification of storms on average is nearly independent of storm duration.

6 Conclusions

Atlantic–European windstorms were identified in the archived dataset of the ECMWF Ensemble Prediction System (EPS) forecasts in the period December 1992 to January 2010. The identification of windstorms was based on the excess over the local 98th percentile of wind speeds (Leckebusch et al., 2008), only taking into account events which have a minimum extension in a single archived time step, and a minimum duration of 24 h (with fulfillment of the minimum extension criterion in each of them). The fact that the operational EPS changed its characteristics to the value of the 98th percentile required that a homogenization procedure was applied to 4 sub periods characterized by different spatial resolutions of the system. Temporal variation of the percentile due to climatic variations and variations with respect to the cubic excess over the percentile (assumed to be model version specific) were taken into account. A diurnal cycle in the 98th percentile of the 10 m wind speed was observed in the EPS, which is also present in ERA-Interim. These diurnal variations comprise a systematically higher value of the threshold percentile for the 12:00 UTC only, which are about 1 $\mathrm{m\,s^{-1}}$ larger than the respective values at the other 6 hourly time steps. This effect also leads to a diurnal variation in the number of storms initiations and ends. Averaged over a large number of storms, this diurnal variation can be seen in the severity at different times of a day. This behavior is, however, partly hidden in the EPS with T_L255 resolutions, as these forecasts have an 18 h periodicity in the threshold for individual time steps presumably assigned to the specific stochastical perturbations imposed in the ensemble generating process during the respective period. None of these effects did have an apparent strong impact on the subsequent evaluations of the EPS as all forecast time steps inside a 6 days window were taken into account. The overall EPS storm properties were found to be similar to ERA-Interim storm properties. In the average the EPS produces the same number of storm days as ERA-Interim. There is no systematic tendency in the total number of storms. The EPS produces developments of storms, which have no observational counterpart. While the principal statistical properties are the same as for modifications of modified representatives of real storms, their share in the total number increases with increasing lead time. They have a spatial distribution of occurrence different from the observed and modified storm, with a focus on the Mediterranean and Eastern Europe. The statistics of the storms indicates a clear increase of maximum intensity and extension of Atlantic–European storms with their duration. This result from the EPS cannot be obtained easily from Reanalysis as the number of very strong events is too low to provide stable statistics. As the spatial distribution, the number of events, the size and duration of events of same severity is in good agreement with real storm events, the EPS can be used to increase the sample size for European winter storm studies by a factor up to number of ensemble member, initializations per day and forecast time. As we used 50 perturbed members and six forecast days, we get a sample size increase of 300 times. For estimations of return periods it has to be taken into account that storm representations are not statistical independent. They are also limited to climate conditions (e.g. SSTs) during the 10 year period considered. Still, the consideration of EPS storms enables us to estimate the potential for an occurrence of storms more extreme than observed based on a physical modeling approach. Compared to estimating return periods of extreme storms from statistics based on observed events, the basis of return periods is much larger and thus the respective estimations have less uncertainty. Summing up, the EPS shows realistic storm properties with a wide range of modifications in the storm properties, where storms can be found with a higher possible impact than appeared as in reality, thus the ability to use this dataset for statistical studies is given.

Acknowledgements. For the possibility to carry out this study we would like to thank the Munich Re for their financial support. We are also grateful to the German Weather Service (DWD) and the ECMWF for providing access to the EPS data and ERA-Interim Reanalysis.

References

Boé, J., Terray, L., Habets, F., and Martin, E.: Statistical and dynamical downscaling of the Seine basin climate for hydro-meteorological studies, Int. J. Climatol., 27, 1643–1655, doi:10.1002/joc.1602, 2007. 1237

Bouttier, F. and Rabier, F.: The operational implementation of 4D-Var, ECMWF Newslett., 78, 2–6, 1997. 1235

Buizza, R. and Hollingsworth, A.: Storm prediction over Europe using ECMWF ensemble prediction system, Meteorol. Appl., 9, 289–305, doi:10.1017/S1350482702003031, 2002. 1233

Dee, D. P., Uppala, S. M., Simmons, A. J., Berrisford, P., Poli, P., Kobayashi, S., Andrae, U., Balmaseda, M. A., Balsamo, G., Bauer, P., Bechtold, P., Beljaars, A. C. M., van de Berg, L., Bidlot, J., Bormann, N., Delsol, C., Dragani, R., Fuentes, M., Geer, A. J., Haimberger, L., Healy, S. B., Hersbach, H., Holm, E. V., Isaksen, L., Kallberg, P., Köhler, M., Matricardi, M., McNally, A. P., Monge-Sanz, B. M., Morcrette, J.-J., Park, B.-K., Peubey, C., de Rosnay, P., Tavolato, C., Thepaut, J.-N., and Vitart, F.: The ERA-Interim reanalysis: configuration and performance of the data assimilation system, Q. J. Roy. Meteor. Soc., 137, 553–597, doi:10.1002/qj.828, 2011. 1234

Della-Marta, P. M., Mathis, H., Frei, C., Liniger, M. A., Kleinn, J., and Appenzeller, C.: The return period of wind storms over Europe, Int. J. Climatol., 29, 437–459, doi:10.1002/joc.1794, 2009. 1233

Dukes, M. D. G. and Palutikof, J. P.: Estimation of extreme wind speeds with very long return periods, J. Appl. Meteorol., 34, 1950–1961, doi:10.1175/1520-0450(1995)034<1950:EOEWSW>2.0.CO;2, 1995. 1233

Froude, L. S. R.: The Predictability of Storm Tracks, PhD thesis, University of Reading, Environmental Systems Science Center, available at: http://www.nerc-essc.ac.uk/~lsrf/Downloads/thesis.pdf (last access: 2 April 2012), 2006. 1233

Froude, L. S. R.: Regional differences in the prediction of extratropical cyclones by the ECMWF ensemble prediction system, Mon. Weather Rev., 137, 893–911, 2009. 1233

Froude, L. S. R. and Gurney, R.: Storm prediction research and its application to the oil/gas industry, in: NATO Science for Peace and Security Series C: Environmental Security, edited by: Troccoli, A., Springer Netherlands, 241–252, doi:10.1007/978-90-481-3692-6_16, 2010. 1234

Hodges, K. I.: A general method for tracking analysis and its application to meteorological data, Mon. Weather Rev., 122, 2573–2586, doi:10.1175/1520-0493(1994)122<2573:AGMFTA>2.0.CO;2, 1994. 1233

Hofherr, T. and Kunz, M.: Extreme wind climatology of winter storms in Germany, Clim. Res., 41, 105–123, 2010. 1233

Klawa, M. and Ulbrich, U.: A model for the estimation of storm losses and the identification of severe winter storms in Germany, Nat. Hazards Earth Syst. Sci., 3, 725–732, doi:10.5194/nhess-3-725-2003, 2003. 1236

Klinker, E., Rabier, F., Kelly, G., and Mahfouf, J.-F.: The ecmwf operational implementation of four-dimensional variational assimilation, III: Experimental results and diagnostics with operational configuration, Q. J. Roy. Meteorol. Soc., 126, 1191–1215, doi:10.1002/qj.49712656417, 2000. 1235

Koziar, C. and Renner, V.: MUSE modellgestützte Untersuchungen zu Sturmfluten mit sehr geringen Eintrittswahrscheinlichkeiten – Teilprojekt: Numerische Berechnung physikalisch konsistenter Wetterlagen mit Atmosphärenmodellen, Tech. rep., DWD, available at: www.bsh.de/de/Meeresdaten/Projekte/MUSE/MUSE_Abschlussbericht.pdf (last access: 22 April 2012), 2005. 1234

Lamquin, N., Gierens, K., Stubenrauch, C. J., and Chatterjee, R.: Evaluation of upper tropospheric humidity forecasts from ECMWF using AIRS and CALIPSO data, Atmos. Chem. Phys., 9, 1779–1793, doi:10.5194/acp-9-1779-2009, 2009. 1238

Lapworth, A.: The evening wind, Weather, 63, 12–14, doi:10.1002/wea.167, 2008. 1239

Title Page
Abstract | Introduction
Conclusions | References
Tables | Figures
◀| |▶
◀ ▶
Back | Close
Full Screen / Esc
Printer-friendly Version
Interactive Discussion

Lapworth, A.: Forecasting the wind at sunset, Weather, 67, 65–67, doi:10.1002/wea.880, 2012. 1239

Leckebusch, G. C., Koffi, B., Ulbrich, U., Pinto, J. G., Spangehl, T., and Zacharias, S.: Analysis of frequency and intensity of European winter storm events from a multi-model perspective, at synoptic and regional scales, Clim. Res., 31, 59–74, 2006. 1233

Leckebusch, G. C., Renggli, D., and Ulbrich, U.: Development and application of an objective storm severity measure for Northeast Atlantic region, Meteorol. Z., 17, 575–587, 2008. 1236, 1240, 1245

Mahfouf, J.-F. and Rabier, F.: The ECMWF operational implementation of four-dimensional variational assimilation, II: Experimental results with improved physics, Q. J. Roy. Meteorol. Soc., 126, 1171–1190, doi:10.1002/qj.49712656416, 2000. 1235

Maraun, D.: Bias correction, quantile mapping, and downscaling: revisiting the inflation issue, J. Climate, 26, 2137–2143, doi:10.1175/JCLI-D-12-00821.1, 2013. 1237

Molteni, F., Buizza, R., Palmer, T. N., and Petroliagis, T.: The ECMWF ensemble prediction system: methodology and validation, Q. J. Roy. Meteorol. Soc., 122, 73–119, doi:10.1002/qj.49712252905, 1996. 1235

Münchener Rückversicherungs-Gesellschaft, Geo Risks Research, N.: Significant natural catastrophes 1980–2011; 10 costliest winter storms in Europe ordered by overall losses, available at: http://www.munichre.com/site/corporate/get/documents_E-1571408806/mr/assetpool.shared/Documents/0_Corporate_Website/_NatCatService/Significant_natural_catastrophes/2011/natcatservice_significant_winter_storms_ins_june2011_touch_en.pdf (last access: 5 February 2015), 2011. 1233

Palmer, T., Molteni, F., Mureau, R., Buizza, R., Chapelet, P., and Tribbia, J.: Ensemble prediction, Technical Memorandum 188, European Centre for Medium Range Weather Forecasts, available at: http://old.ecmwf.int/publications/library/ecpublications/_pdf/tm/001-300/tm188.pdf (last access: 10 April 2012), 1992. 1235

Palmer, T. N., Buizza, R., Leutbecher, M., Hagedorn, R., Jung, T., Rodwell, M., Vitart, F., Berner, J., Hagel, E., Lawrence, A., Pappenberger, F., Park, Y.-Y., von Bremen, L., and Gilmour, I.: The Ensemble Prediction System – recent and ongoing developments, Technical Memorandum 540, European Centre for Medium Range Weather Forecasts, paper presented to the 36th Session of the SAC, 8–10 October 2007, available at: http://www.aosc.umd.edu/~ekalnay/syllabi/AOSC614/PalmerENStm540.pdf (last access: 5 July 2011), 2007. 1235

Title Page
Abstract | Introduction
Conclusions | References
Tables | Figures
◀| |▶
◀ ▶
Back | Close
Full Screen / Esc
Printer-friendly Version
Interactive Discussion

Rabier, F., Järvinen, H., Klinker, E., Mahfouf, J.-F., and Simmons, A.: The ECMWF operational implementation of four-dimensional variational assimilation. I: Experimental results with simplified physics, Q. J. Roy. Meteorol. Soc., 126, 1143–1170, doi:10.1002/qj.49712656415, 2000. 1235

Roberts, J. F., Champion, A. J., Dawkins, L. C., Hodges, K. I., Shaffrey, L. C., Stephenson, D. B., Stringer, M. A., Thornton, H. E., and Youngman, B. D.: The XWS open access catalogue of extreme European windstorms from 1979 to 2012, Nat. Hazards Earth Syst. Sci., 14, 2487–2501, doi:10.5194/nhess-14-2487-2014, 2014. 1233

Table 1. Overview of general characteristics of the EPS (*used temporal resolution*) pf: perturbed forecast; cf: control forecast.

Time Frame	Spatial Resolution	Temporal Resolution [h]	Number of Member	Initialisations at
21 Nov 1992–9 Dec 1996	T63	12 (*12*)	32pf + 1cf	12:00 UTC
10 Dec 1996–20 Nov 2000	T_L159	12 and 6 (*12*)	50pf + 1cf	12:00 UTC
21 Nov 2000–31 Jan 2006	T_L255	6 and 3 (*6*)	50pf + 1cf	00:00 and 12:00 UTC
1 Feb 2006–25 Jan 2010	T_L399	3 (*6*)	50pf + 1cf	00:00 and 12:00 UTC

Discussion Paper | Discussion Paper | Discussion Paper | Discussion Paper |

Table 2. Average storm properties of EPS (ERA-Interim).

Resolution	No. per year	Size [10^6 km^2]	Duration [h]
T_L159 (12 hourly)	45.9 (49.3)	0.75 (0.79)	49.2 (50.4)
T_L255 (6 hourly)	47.6 (45.0)	0.71 (0.76)	41.4 (42.0)
T_L399 (6 hourly)	47.9 (50.5)	0.74 (0.74)	42.0 (42.6)

Table 3. Parameters and their errors of fitted normal distribution to logarithmic of SSI for the EPS using both scaling techniques together and ERA-Interim.

Model	Mean	Std	Error mean	Error std
ERA (period of EPS T_L255)	0.73	1.30	0.077	0.055
EPS T_L255	0.77	1.32	0.003	0.002
ERA (period of EPS T_L399)	0.72	1.35	0.086	0.061
EPS T_L399	0.76	1.33	0.005	0.004

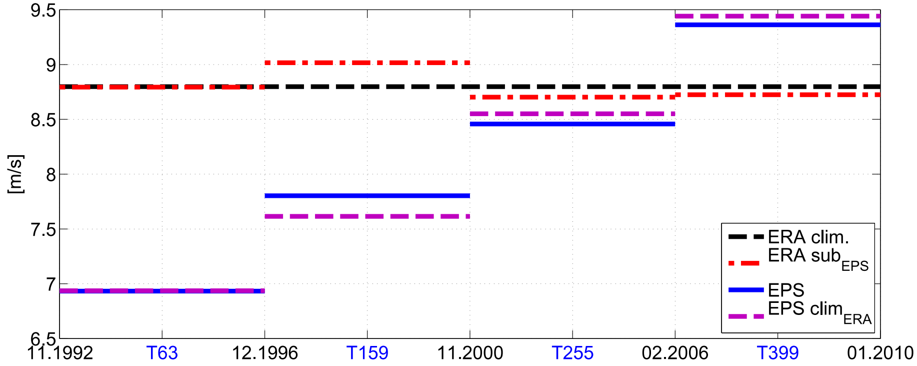

Figure 1. 98th percentile as average over land boxes for different EPS sub periods with corresponding 98th ERA-Interim percentile.

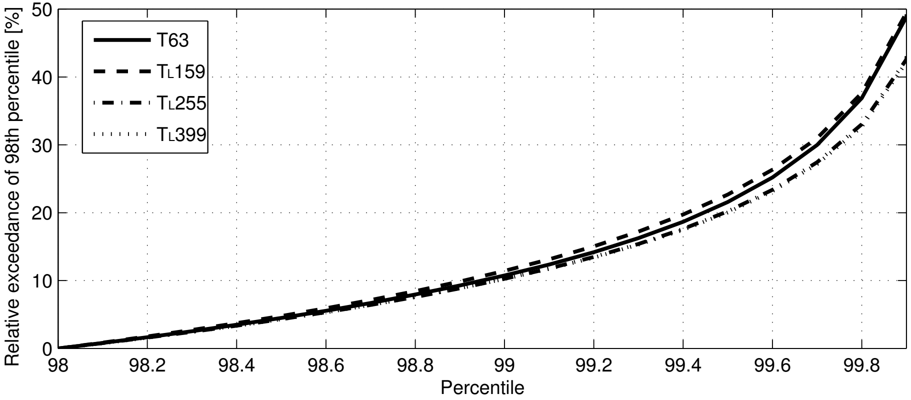

Figure 2. Visualization of tail differences in the wind speed distribution of the four subperiods (see Table 1) of the EPS. Shown: relative exceedance of 98th EPS percentile as land average. Internal climate variability of the disjunct periods is excluded by utilization of the climatological scaling (for details see text).

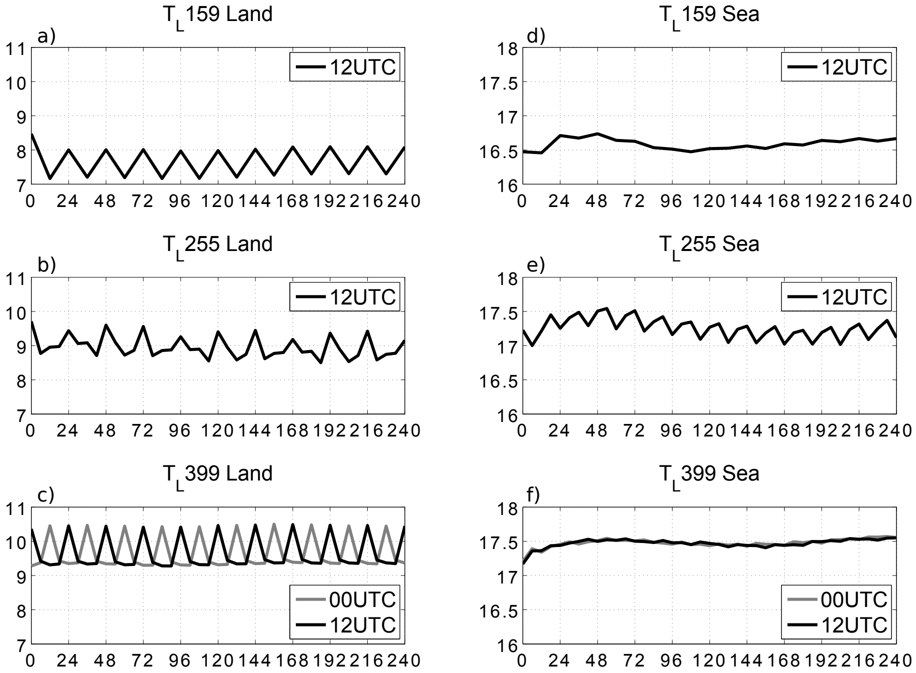

Figure 3. Average of 98th percentile [m/s] for different forecast lead times (right axis, [h] after initialization): for T_L159 12 hourly **(a, d)**, T_L255 **(b, e)** and T_L399 6 hourly **(c, f)**. **(a)–(c)** for land grid boxes, **(d)–(f)** for sea grid boxes.

Title Page
Abstract | Introduction
Conclusions | References
Tables | Figures
◀| |▶
◀ ▶
Back | Close
Full Screen / Esc
Printer-friendly Version
Interactive Discussion

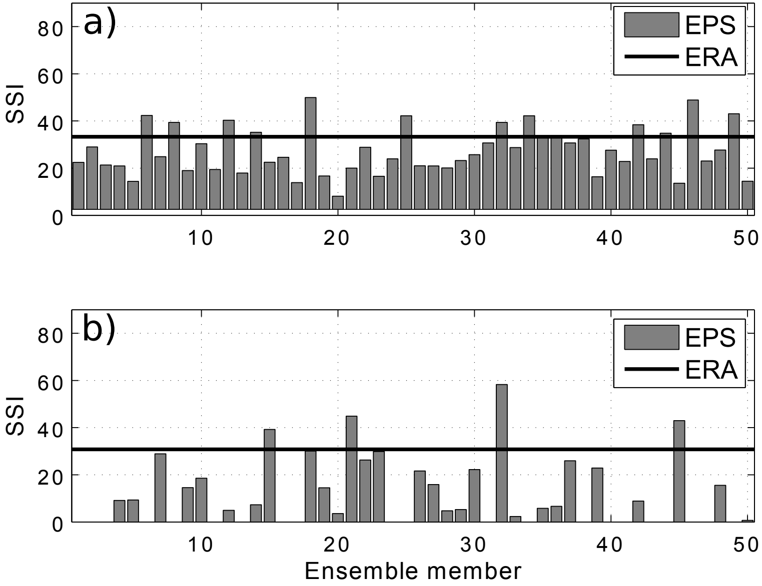

Figure 4. SSIs for representations of storm Emma (28 February 2008 18:00 UTC detected in ERA-Interim) in 50 EPS member **(a)** 6 h lead time, initialized 28 February 2008, 12:00 UTC and **(b)** 90 h lead time, initialized 25 February 2008, 00:00 UTC.

Title Page
Abstract
Introduction
Conclusions
References
Tables
Figures
I◄
►I
◄
►
Back
Close
Full Screen / Esc
Printer-friendly Version
Interactive Discussion

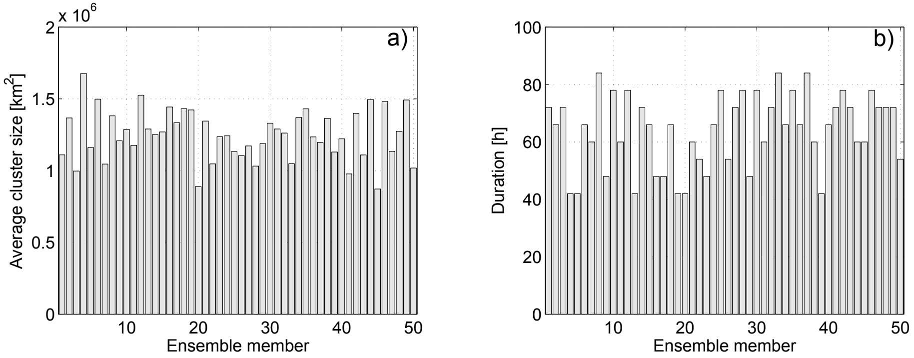

Figure 5. (a) Average cluster size [km^2] for storm representation Emma (28 February 2008 18:00 UTC detected in ERA-Interim) in 50 EPS member initialized 28 February 2008 12:00 UTC **(b)** duration [h].

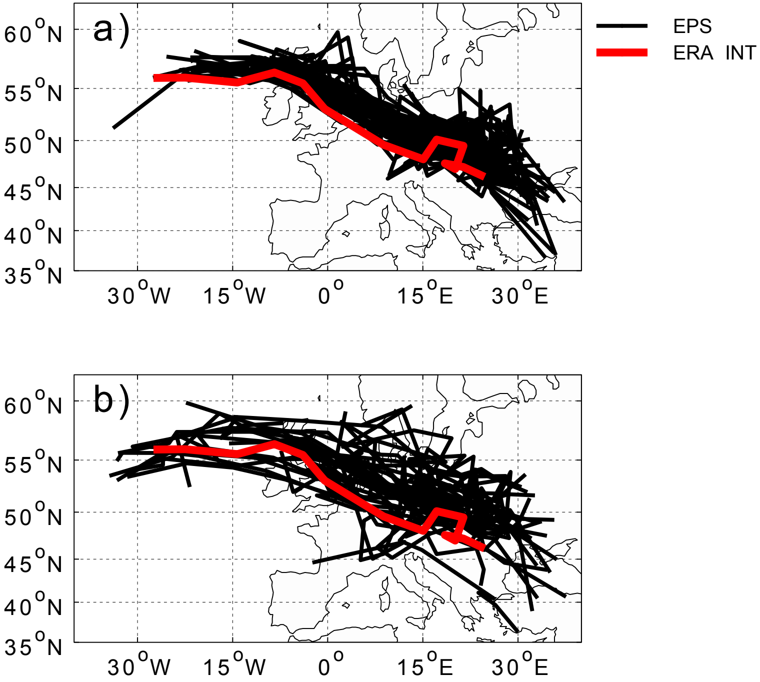

Figure 6. Tracks for representations of storm Emma (28 February 2008 18:00 UTC detected in ERA-Interim) in 50 EPS member initialized for **(a)** 28 February 2008 12:00 UTC and **(b)** 25 February 2008 00:00 UTC.

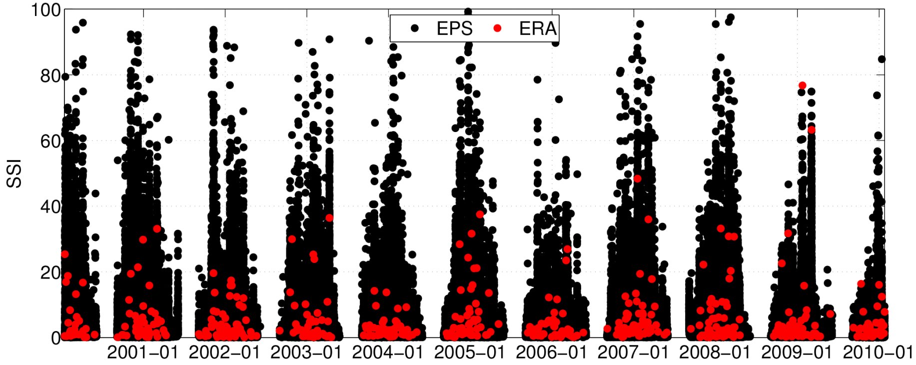

Figure 7. SSIs for all storms in ERA-Interim in 2001 to 2010 and for the EPS in 2001 to 2010 with initializations at 12:00 UTC.The months June, July and August are excluded.

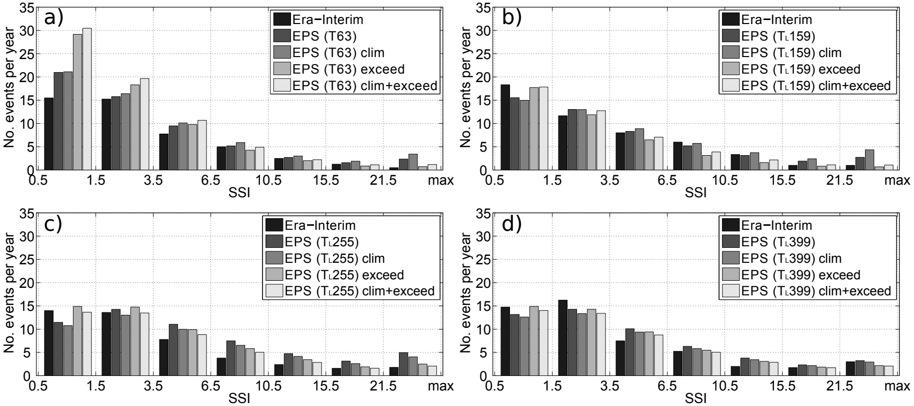

Figure 8. No. of storm events per year subdivided according to the severity, for the four individual sub periods with constant horizontal resolution **(a)** T63 **(b)** T_L159 **(c)** T_L255 **(d)** T_L399 of the EPS. (T63 and T_L159 in 12 hourly resolution for EPS and ERA-Interim.) First bar is for ERA-Interim, the other for the EPS (bars from left to right: 2nd) EPS raw data, 3rd) processed by climatological scaling, 4th) processed by scaling of exceedance and 5th) applying both scaling techniques on the data.

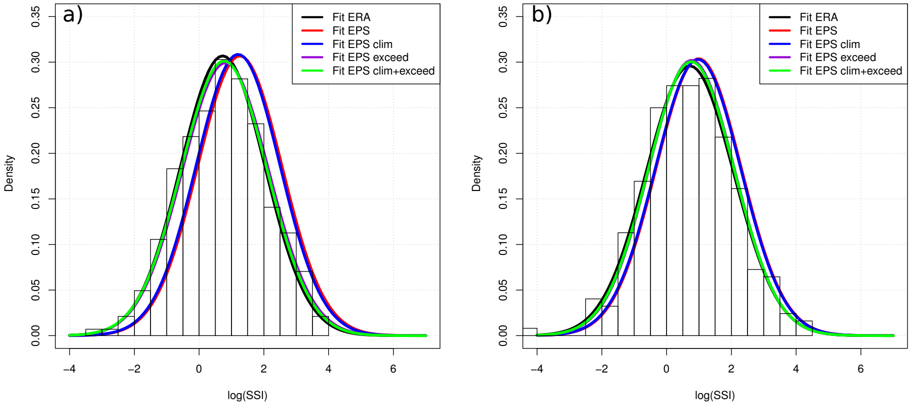

Figure 9. Fit of normal distributions to logarithmic of SSI for **(a)** EPS in T_L255 and **(b)** EPS in T_L399 without scaling techniques, climatological scaling, exceedance scaling and both scaling techniques together.

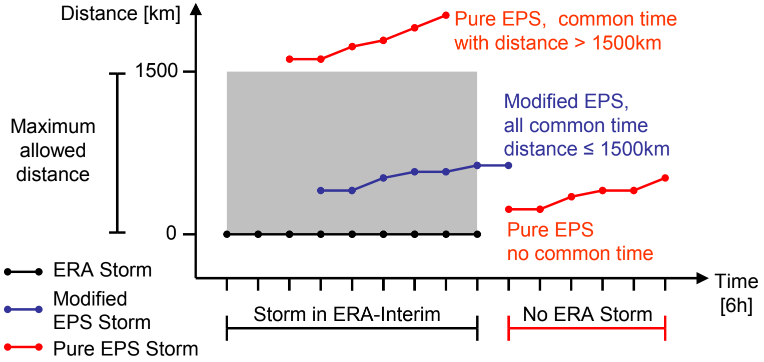

Figure 10. Sketch of Definition for “pure” and “modified” EPS storms.

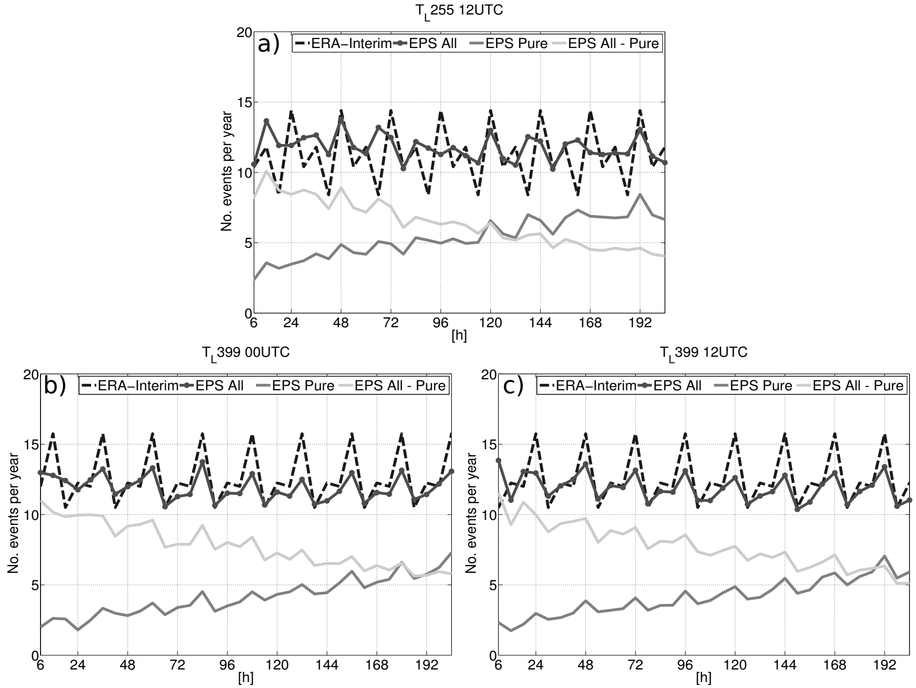

Figure 11. Temporal evolution of the number of first storm detections during the integration time [h] after initialization **(a)** T$_L$255 – 12:00 UTC, **(b)** T$_L$399 – 00:00 UTC, **(c)** T$_L$399 – 12:00 UTC.

Title Page
Abstract
Introduction
Conclusions
References
Tables
Figures
◀|
|▶
◀
▶
Back
Close
Full Screen / Esc
Printer-friendly Version
Interactive Discussion

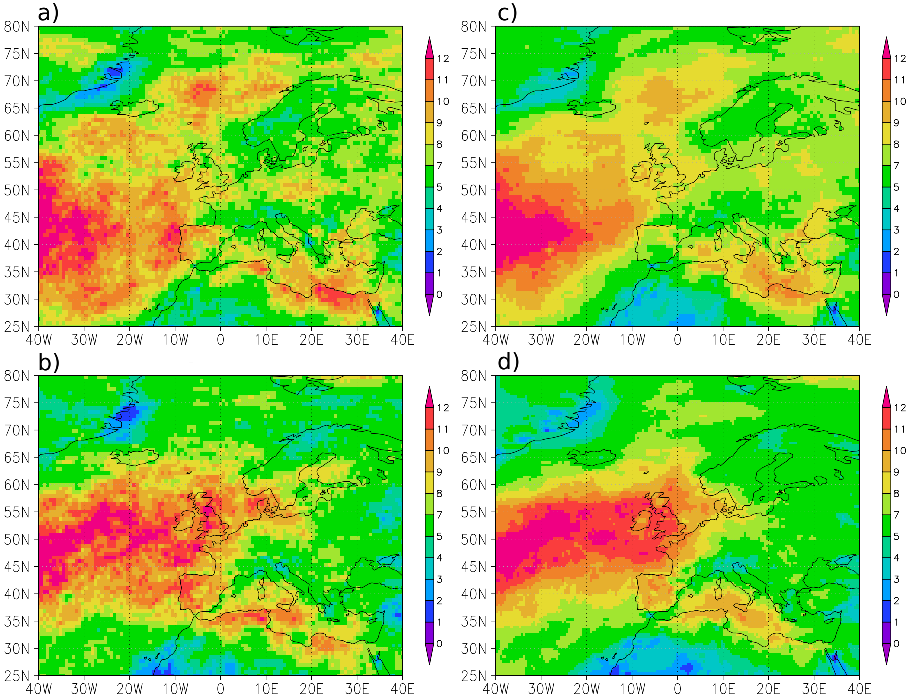

Figure 12. Cumulative area affection by detected storms (sum of footprints per year) for time frame of the EPS resolution T_L255 (**a** and **c**) and T_L399 (**b** and **d**), ERA (**a** and **b**), EPS (**c** and **d**) normed by ensemble size (right).

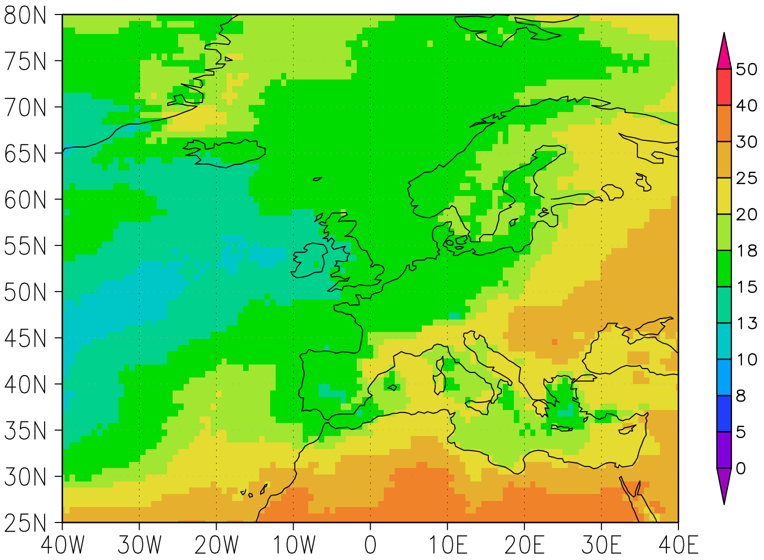

Figure 13. Relative grid cell affection [%] by pure EPS storms for EPS with T_L255 initialized at 12:00 UTC.

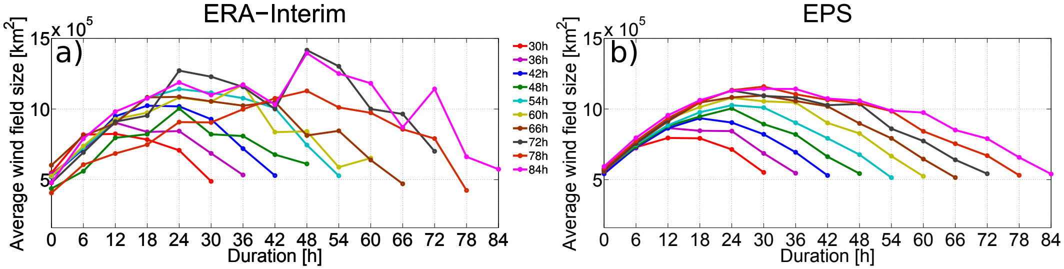

Figure 14. Wind field size during storm duration for storm duration between 30 and 84 h; **(a)** for ERA-Interim and **(b)** for the EPS.

Title Page
Abstract Introduction
Conclusions References
Tables Figures
◀◀ ▶▶
◀ ▶
Back Close
Full Screen / Esc
Printer-friendly Version
Interactive Discussion

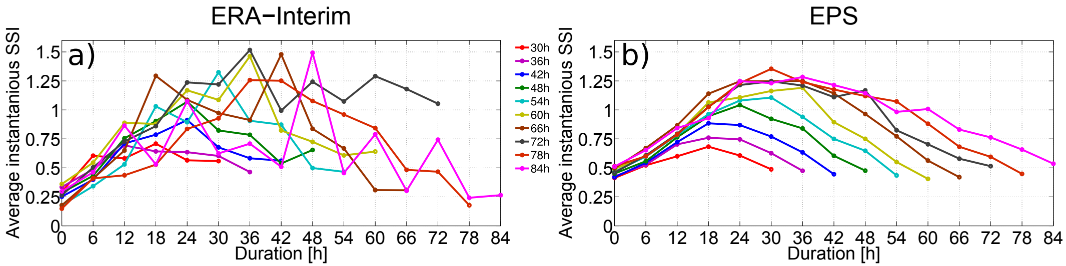

Figure 15. Storm severity during storm duration for storm duration between 30 and 84 h; **(a)** for ERA-Interim and **(b)** for the EPS.